Optimization of the electrical asymmetry effect in dual-frequency capacitively coupled radio frequency discharges: Experiment, simulation, and model

J. Schulze,[1,a)] E. Schüngel,[1] U. Czarnetzki,[1] and Z. Donkó[2]
[1]*Institute for Plasma and Atomic Physics, Ruhr-University Bochum, 44780 Bochum, Germany*
[2]*Research Institute for Solid State Physics and Optics, Hungarian Academy of Sciences, 1525 Budapest POB 49, Hungary*

(Received 25 June 2009; accepted 4 August 2009; published online 24 September 2009)

An electrical asymmetry in capacitive rf discharges with a symmetrical electrode configuration can be induced by driving the discharge with a fundamental frequency and its second harmonic. For equal amplitudes of the applied voltage waveforms, it has been demonstrated by modeling, simulation, and experiments that this electrical asymmetry effect (EAE) leads to the generation of a variable dc self-bias that depends almost linearly on the phase angle between the driving voltage signals. Here, the dependence of the dc self-bias generated by the EAE on the choice of the voltage amplitudes, i.e., the ratio A of high to low frequency amplitude, is investigated experimentally as well as by using an analytical model and a particle-in-cell simulation. It is found that (i) the strongest electrical asymmetry is induced for $A<1$ at pressures ranging from 6 to 100 Pa and that (ii) around this optimum voltage ratio the dc self-bias normalized to the sum of both voltage amplitudes is fairly insensitive to changes of A. Thus, by choosing the optimum voltage ratio, the EAE is optimized: The ion energy can be changed over a broader energy range and a high degree of process stability with respect to small changes in the applied voltages is expected.
 [doi:10.1063/1.3223310]

I. INTRODUCTION

Capacitively coupled radio frequency (CCRF) discharges are frequently used for a variety of applications, e.g., chip and solar cell manufacturing, as well as for the creation of biocompatible surfaces. For these applications, separate control of ion energy and ion flux at the electrode surfaces is essential.[1] Dual-frequency CCRF discharges operated at two substantially different frequencies (e.g. 2+27 MHz) are usually used to achieve this separate control.[2–6] However, recent investigations have shown that there can be a strong coupling between the two frequencies, which might limit this separate control.[7–13]

In asymmetric discharges, the dc self-bias η affects the energy of ions reaching the electrodes since the ion energy at a given electrode is generally determined by the mean voltage drop across the sheath adjacent to this electrode. A discharge asymmetry can be created in two different ways: (i) a geometric asymmetry caused by different electrode surface areas and/or (ii) an electrical asymmetry caused by driving the discharge with a voltage waveform, of which the absolute values of the positive and negative extrema are different. The former method is well known[1,14–20] but practically does not allow to adjust the dc self-bias without changing the amplitude of the applied rf voltage waveform. A different voltage amplitude, however, will change the ion flux. Thus, this method does not allow separate control of ion energy and flux. The latter method is based on the recently discovered electrical asymmetry effect (EAE) in dual-frequency CCRF discharges operated at a fundamental frequency and its second harmonic.[21–27] The EAE allows to change η even in geometrically symmetric discharges by adjusting the phase angle between the two applied voltage waveforms without changing their amplitudes. Therefore, the ion energy can be controlled separately from the ion flux. The control parameter is the phase angle. At equal amplitudes of high and low frequency harmonics, the EAE and the related separate control of ion energy and flux have been investigated experimentally[25] as well as by using an analytical model,[22,23] a hybrid fluid Monte Carlo simulation,[21–24] and a particle-in-cell (PIC) simulation.[23,24,26] It has been demonstrated that the EAE induces a variable dc self-bias, which is an almost linear function of the phase angle. However, until now the investigations of the EAE (Refs. 21–26) have been restricted to a superposition of two rf voltage waveforms (fundamental +second harmonic) with identical amplitudes of each harmonic. Thus, two fundamental questions most relevant to applications remain: (i) What is the optimum choice of amplitudes for each voltage harmonic to induce the strongest electrical discharge asymmetry? (ii) How sensitive is the dc self-bias generated by the EAE to changes in the amplitudes of each voltage harmonic? These questions are most relevant for applications since a higher electrical discharge asymmetry provides the opportunity to change the ion energy over a wider energy range by adjusting the phase and since a high degree of process stability is required for applications; i.e., the ion energy should not change drastically if the amplitudes of both applied voltage harmonics are changed by a few percent.

[a)]Electronic mail: fjschulze@hotmail.com.

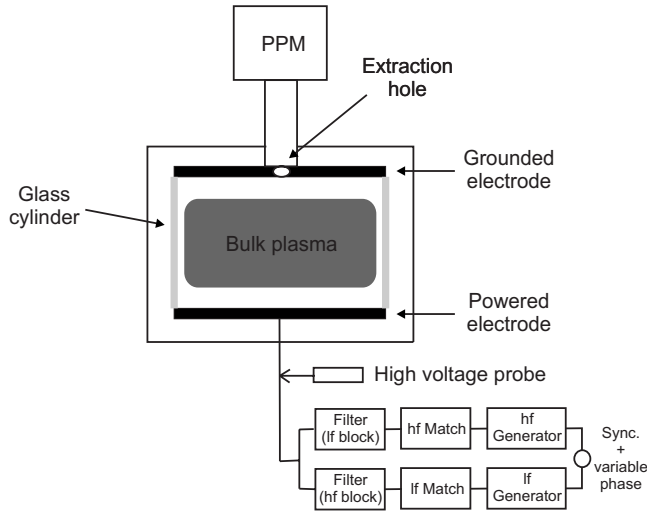

FIG. 1. Experimental setup (Ref. 25): The PPM is not used for the investigations presented here.

In this work, these two questions are answered: We investigate a geometrically symmetric dual-frequency CCRF discharge operated at 13.56 and 27.12 MHz with a variable phase shift θ between the voltage harmonics experimentally, by a PIC simulation, and by an analytical model.[22] We keep the amplitude of the 13.56 MHz harmonic, ϕ_{lf}, constant and vary the amplitude of the 27.12 MHz component, ϕ_{hf}, at $0 \leq \phi_{\mathrm{hf}} \leq 2\phi_{\mathrm{lf}}$; i.e., we vary the ratio of the high and low frequency voltage amplitudes. We measure and calculate (by a PIC simulation and an analytical model) the dc self-bias normalized to the sum of both voltage amplitudes as a function of this amplitude ratio $A=\phi_{\mathrm{hf}}/\phi_{\mathrm{lf}}$. It will be demonstrated that (i) the strongest normalized dc self-bias $\bar{\eta}=\eta/(\phi_{\mathrm{lf}}+\phi_{\mathrm{hf}})$ is not generated at equal voltage amplitudes such as those used in previous works, but at $A<1$, and that (ii) the normalized dc self-bias is relatively insensitive to changes in the voltage amplitudes around its optimum value providing a high degree of process stability.

II. EXPERIMENTAL SETUP

The experimental setup is shown in Fig. 1. It is the same setup as for the investigations of separate control of ion energy and ion flux via the EAE using $A=1$ (equal voltage amplitudes).[25] Thus, only a brief description is given here: Two synchronized function generators are used to generate the fundamental frequency and its second harmonic with an adjustable phase angle between them. Both frequencies are amplified and matched individually. Behind each matchbox, a filter blocks the other harmonic. The superposition of both voltage waveforms,

$$\tilde{\phi} = \phi_{\mathrm{lf}} \cos[\varphi(t) + \theta] + \phi_{\mathrm{hf}} \cos[2\varphi(t)], \tag{1}$$

is then applied to the bottom electrode of a modified gaseous electronics conference (GEC) cell of which the upper electrode is grounded.

Here, $\varphi(t)=2\pi ft$, with $f=13.56$ MHz. The diameter of the electrodes is 10 cm. The discharge is operated in argon. The plasma is shielded from the outer grounded chamber walls by a cylindrical glass tube to improve the geometrical symmetry of the discharge. Thus, the discharge is approximately geometrically symmetric. The plasma process monitor (PPM) is not used for the investigations presented here. Measurements of η as a function of θ and A at 100 Pa are performed with an electrode gap $d=1$ cm. At larger electrode gaps, the bad aspect ratio between the electrode diameter and the gap causes capacitive coupling between the glass cylinder and the outer grounded chamber wall. This capacitive coupling to ground results in an effective enlargement of the grounded surface and, therefore, leads to an additional geometrical asymmetry, which causes an additional negative dc self-bias.[14,16,25] Due to this asymmetry at larger gaps, the measured dc self-bias cannot be compared to simulations and models of perfectly geometrically symmetric discharges with larger electrode gaps. For such a comparison, electrodes with a significantly larger radius would be required.

The voltage waveform is measured by a LeCroy high voltage probe about 1.5 m in front of the electrode. The amplitude of each individual harmonic is determined by a Fourier analysis of the measured superposition. Due to reflection on the cable, the voltage amplitudes and the phase θ between the harmonics are different at the electrode and at the position in front of the electrode, where the voltage is measured during discharge operation. In order to determine the voltage amplitudes and the phase shift at the electrode, the same calibration procedure as described in Ref. 25 is applied: When the chamber is vented (no plasma), the voltage is measured directly at the electrode and at the position, where the voltage is measured during the plasma operation. From a comparison of these two voltage values, the phase shift and the calibration factors for both voltage amplitudes are determined. In the experiment, the amplitude of the low frequency voltage waveform is kept constant at $\phi_{\mathrm{lf}}=50$ V.

III. PIC SIMULATION

The simulation used in this work is a one-dimensional (1d3v) bounded plasma PIC simulation complemented with a Monte Carlo treatment of collision processes. At the planar, parallel, and infinite electrodes, electrons are reflected with a probability of 20%, and the secondary electron coefficient is $\gamma=0$. The cross sections for electron-neutral and ion-neutral collision processes are taken from Refs. 28–30. The dc self-bias is determined in an iterative way to ensure that the charged particle fluxes to the two electrodes, averaged over one low frequency period, become equal. Details of the PIC simulation can be found elsewhere.[13,24,31,32] The simulations are performed for two different electrode gaps of $d=1$ cm and $d=2.5$ cm. Similar to the experiment, the discharge is driven by the voltage waveform given by Eq. (1). The amplitude of the low frequency voltage is kept constant at $\phi_{\mathrm{lf}}=50$ V in the case of the 1 cm electrode gap and at $\phi_{\mathrm{lf}}=100$ V in the case of the 2.5 cm electrode gap. For $d=1$ cm and 100 Pa, η is determined as a function of θ and A. In this case, identical conditions are used in the experiment and in the simulation, and the results are compared to each other. For $d=2.5$ cm, η is only calculated at $\theta=0°$ as a function of A for 6, 10, and 100 Pa.

IV. ANALYTICAL MODEL

The analytical model is the same as that introduced in Ref. 22. Under the assumptions of negligible voltage drop across the plasma bulk, a temporally constant net positive charge in the discharge, and that both sheaths totally collapse at least once per rf period, the following expression for the dc self-bias η has been derived:[22]

$$\eta = -\frac{\tilde{\phi}_{m1} + \varepsilon\tilde{\phi}_{m2}}{1+\varepsilon}. \tag{2}$$

$\tilde{\phi}_{m1}$ and $\tilde{\phi}_{m2}$ are the maximum and the minimum of the applied voltage waveform $\tilde{\phi}$, respectively, and ε is the symmetry parameter,

$$\varepsilon = \left|\frac{\hat{\phi}_{sg}}{\hat{\phi}_{sp}}\right|. \tag{3}$$

Here, $\hat{\phi}_{sg}$ and $\hat{\phi}_{sp}$ are the maximum sheath voltages across the sheath at the grounded and powered electrodes, respectively. The model[22] predicts the most negative dc self-bias at $\theta \approx 0°$. For this phase angle, the extrema $\tilde{\phi}_{m1}$ and $\tilde{\phi}_{m2}$ of Eq. (1) are calculated and then substituted into Eq. (2) to calculate η. At $A=1/4$, a transition occurs: For $A<1/4$, Eq. (1) has one maximum and one minimum per low frequency rf period. For $A>1/4$, Eq. (1) still has only one maximum but two minima of the same modulus per low frequency rf period. The maximum $\tilde{\phi}_{m1}$ and minimum $\tilde{\phi}_{m2}$ of Eq. (1) are found at the following values of φ_1 and φ_2 for $\varphi(t)$, respectively,

$$A \le \frac{1}{4}: \quad \begin{aligned} &\tilde{\phi}_{m1}: \quad \varphi_1 = 2k\pi, \quad k \in \mathbb{Z}, \\ &\tilde{\phi}_{m2}: \quad \varphi_2 = (2k+1)\pi, \quad k \in \mathbb{Z}, \end{aligned} \tag{4}$$

$$A \ge \frac{1}{4}: \quad \begin{aligned} &\tilde{\phi}_{m1}: \quad \varphi_1 = 2k\pi, \quad k \in \mathbb{Z}, \\ &\tilde{\phi}_{m2}: \quad \varphi_2 = \arccos\left(-\frac{1}{4A}\right) + 2k\pi, \quad k \in \mathbb{Z}. \end{aligned} \tag{5}$$

The substitution of Eqs. (4) and (5) into Eq. (1) yields $\tilde{\phi}_{m1}$ and $\tilde{\phi}_{m2}$, which are then substituted into Eq. (2) to calculate η. Then, the dc self-bias normalized by the sum of the voltage amplitudes is

$$\bar{\eta} = \frac{\eta}{\phi_{lf}+\phi_{hf}} \underset{\theta=0°}{=} -\frac{1-\varepsilon f(A)}{1+\varepsilon}, \tag{6}$$

$$f(A) = \frac{1}{1+A}\begin{cases} 1-A, & A \le \frac{1}{4} \\ A + \frac{1}{8A}, & A \ge \frac{1}{4}. \end{cases} \tag{7}$$

The normalized bias $\bar{\eta}$ depends on ε and $f(A)$. This function $f(A)$ has a minimum at $A=\frac{1}{2}$ and increases only slowly for larger values of A. On the other hand, the absolute value of $\bar{\eta}$ increases monotonically with decreasing ε. Thus, if $\varepsilon=1$ (high pressure conditions), this analytical form yields a maximum bias $\bar{\eta}=\frac{1}{4}$ at $A=\frac{1}{2}$ and not at $A=1$. For $\varepsilon \neq 1$, a calculation of $\bar{\eta}$ is more complicated since ε itself depends on the dc self-bias due to the self-amplification of the EAE, as described in Refs. 22–25. At low pressures, the sheath is collisionless, and, thus, a higher dc self-bias leads to faster ions at one electrode and, consequently, to a smaller mean ion density within the sheath adjacent to this electrode due to flux conservation. This effect changes the symmetry of the discharge and yields an even stronger dc self-bias. The symmetry parameter ε is calculated by the PIC simulation and is used as an input parameter for the analytical model. In this way, $\bar{\eta}$ is calculated as a function of A at 6 and 10 Pa ($d=2.5$ cm). At 100 Pa, $\varepsilon=1$ is assumed, which is well justified by the simulation results, and $\bar{\eta}$ is calculated as a function of θ and A by the analytical model.

V. RESULTS

Figure 2 shows the symmetry parameter ε as a function of the voltage amplitude ratio A resulting from the PIC simulation at $\theta=0°$ for 6, 10, and 100 Pa ($d=2.5$ cm and $\phi_{lf}=100$ V). Due to the self-amplification of the EAE, ε is significantly smaller than unity at low pressures for voltage ratios A, at which a strong dc self-bias is observed. At 100 Pa, ε remains close to unity since the self-amplification is greatly reduced.

For the model calculations, ε resulting from the PIC simulation ($d=2.5$ cm, Fig. 2) is used as an input parameter for Eq. (6) to calculate $\bar{\eta}$ as a function of A. The $\bar{\eta}$ values calculated this way, along with those determined directly from the PIC simulation, are shown in Fig. 3 for $\theta=0°$ and $d=2.5$ cm. Generally, an excellent agreement is found. At all pressures, the self-bias vanishes at $A=0$ since the discharge is geometrically symmetric and operated as a single frequency discharge (low frequency only). With increasing A, the absolute value of the normalized bias $\bar{\eta}$ increases until it reaches a flat maximum at $A_{max}<1$ ($A_{max}\approx 0.7$ at 6 and 10 Pa; $A_{max}\approx 0.6$ at 100 Pa). The value of $A_{max}\approx 0.6$ at 100 Pa agrees well with the model prediction of $A_{max}=0.5$ for $\varepsilon=1$ (see Fig. 2). The difference between these A_{max} values at low and high pressures is caused by the self-amplification of the EAE at low pressures and the related dependence of ε on A

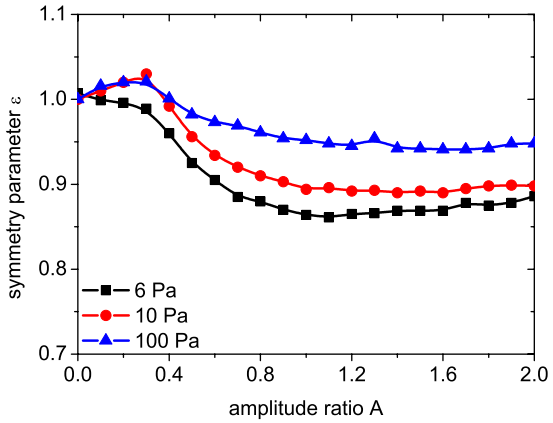

FIG. 2. (Color online) Symmetry parameter ε (calculated by the PIC simulation) as a function of the voltage amplitude ratio A at $\theta=0°$ and at pressures of 6, 10, and 100 Pa ($\phi_{lf}=100$ V and $d=2.5$ cm).

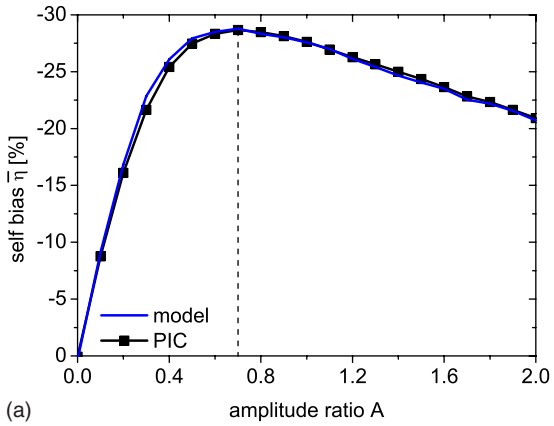

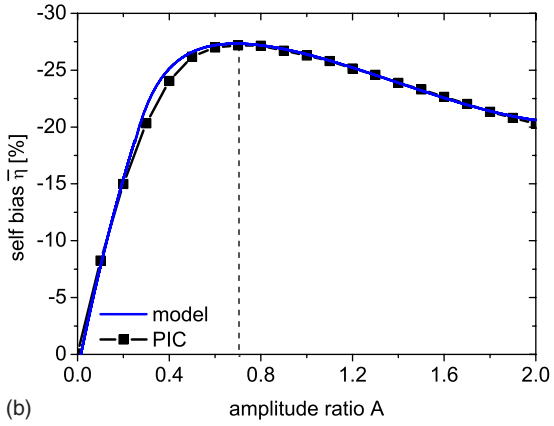

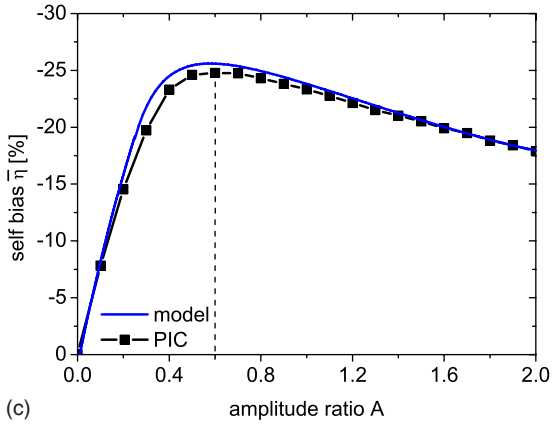

FIG. 3. (Color online) Normalized dc self-bias $\bar{\eta}$ as a function of the amplitude ratio A for $\theta=0°$ resulting from the analytical model and the PIC simulation ($\phi_{lf}=100$ V) at (a) 6 Pa, (b) 10 Pa, and (c) 100 Pa. The vertical dashed lines indicate the maxima of $|\bar{\eta}|$ at $A=A_{max}$.

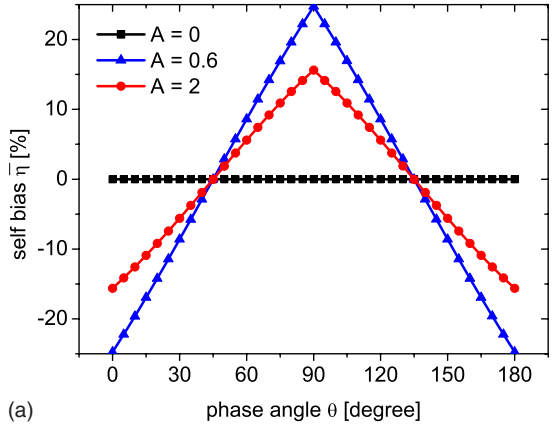

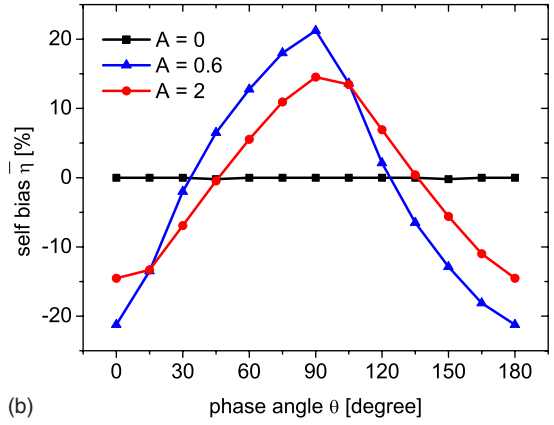

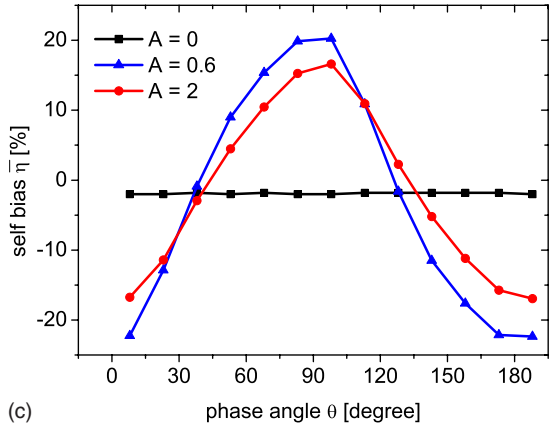

FIG. 4. (Color online) Normalized dc self-bias $\bar{\eta}$ as a function of θ for $A=0$ (single frequency discharge), $A=0.6$ (strong $\bar{\eta}$), and $A=2$ at 100 Pa, $d=1$ cm, and $\phi_{lf}=50$ V resulting from the analytical model assuming (a) $\varepsilon=1$, (b) the PIC simulation, and (c) the experiment.

(see Fig. 2) shifting the maximum of $|\bar{\eta}|$ due to Eq. (6). For the same reason $\bar{\eta}$ is stronger at lower pressures (28.5%, 27%, and 25% at 6, 10, and 100 Pa, respectively). For $A\rightarrow\infty$, $|\bar{\eta}|$ decreases monotonically toward 0 since for very high values of A the geometrically symmetric discharge is again essentially driven by only one frequency (high frequency only). For applications, the most relevant result is the flatness of the maximum of $|\bar{\eta}|$ observed at all pressures. Around the maximum, the normalized self-bias changes by less than 1% if A is changed by 15%. In non-normalized quantities at 6 Pa, this corresponds to a change of 10 V of the amplitude of the hf component ($\phi_{0,lf}=100$ V, $\phi_{0,hf}=70$ V), which causes a change in the self-bias of only about 2.5 V (dc self-bias of 48.7 V at $A=0.7$). This means that the normalized dc self-bias generated by the EAE is very insensitive to small changes in the amplitudes of the applied voltage harmonics. Thus, a high degree of process stability is expected if the ion energy is controlled via the EAE. In order to generate the strongest variable electrical asymmetry, to have optimum control of the ion energy, the discharge should be operated at A_{max} rather than at other voltage amplitude ratios.

Figure 4 shows the normalized dc self-bias $\bar{\eta}$ as a function of θ for $A=0$ (single frequency discharge), $A=0.6$ (strong $\bar{\eta}$), and $A=2$ at 100 Pa, $d=1$ cm, and $\phi_{lf}=50$ V

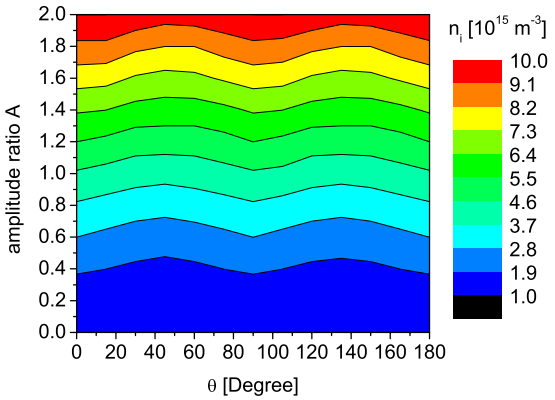

FIG. 5. (Color online) Ion density in the discharge center as a function of θ and A (PIC: 100 Pa, $\phi_{lf}=50$ V, and $d=1$ cm). The color scale shows the ion density in 10^{15} m^{-3}. The ion density increases monotonically as a function of A.

resulting from the analytical model assuming $\varepsilon=1$ (plot a), the PIC simulation (plot b), and the experiment (plot c). By changing θ from 0° to 90°, $\bar{\eta}$ changes from $\bar{\eta}$ (0°) to $\bar{\eta}$ (90°)$=-\bar{\eta}$ (0°) for all values of A investigated; i.e., the role of both electrodes is reversed.[22–25] In contrast to the results of the analytical model and the PIC simulation, in the experiment the dc self-bias is not exactly zero at $A=0$ since the capacitive coupling between the glass cylinder and the outer grounded chamber wall causes a small effective discharge asymmetry even at this short electrode gap.

Figure 5 shows the ion density in the discharge center as a function of θ and A resulting from the PIC simulation at 100 Pa, 1 cm electrode gap, and $\phi_{lf}=50$ V. With increasing amplitude ratio A, more power is applied to the discharge and, consequently, the ion density and the ion flux increase as a function of A at a constant phase angle θ. By increasing A from 0 to 2, the ion density is increased by one order of magnitude. The ion density remains approximately constant within about $\pm 10\%$ as a function of θ at constant A.

Figure 6 shows the normalized dc self-bias $\bar{\eta}$ as a function of θ and A at 100 Pa and 1 cm electrode gap, resulting from the analytical model (plot a), the PIC simulation (plot b), and the experiment (plot c). In the simulation and in the experiment, identical conditions are investigated. In the analytical model, $\varepsilon=1$ is used, which is well justified by the PIC simulation. Again, an excellent agreement between the results of the model, the simulation, and the experiment is found. At all phase angles θ, a dependence of $\bar{\eta}$ on A, similar to the ones shown in Fig. 3, is observed. At a fixed amplitude ratio A dependencies of $\bar{\eta}$ on θ qualitatively similar to the ones shown in Fig. 4 are found. This result shows that a high degree of process stability can be expected at all phase angles θ if the discharge is operated at $A=A_{max}$ and that the ion energy can be controlled effectively via the EAE at all amplitude ratios A investigated.

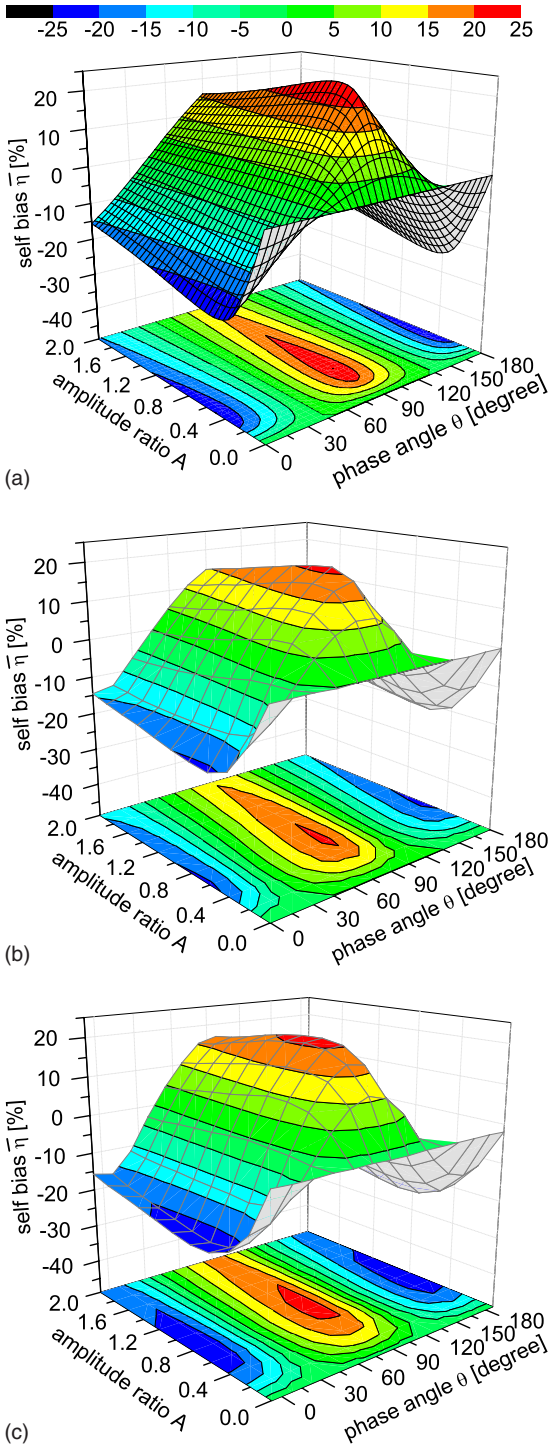

FIG. 6. (Color online) Normalized dc self-bias $\bar{\eta}$ as a function of θ and A at 100 Pa resulting from (a) the analytical model (assuming $\varepsilon=1$), (b) the PIC simulation, and (c) the experiment. $d=1$ cm and $\phi_{lf}=50$ V. The color scale at the top of the figure shows the normalized dc self-bias in percent.

VI. CONCLUSIONS

In conclusion, the dependence of the dc self-bias normalized to the sum of the amplitudes of the applied voltage waveforms on two parameters, the phase angle θ and the ratio of the amplitudes of the applied voltage waveforms A, has been investigated by an analytical model, a PIC simulation, and experimentally. It has been demonstrated that the EAE can be optimized by choosing an amplitude ratio smaller than unity, leading to an even stronger normalized dc self-bias in a geometrically symmetric dual-frequency CCRF discharge. This bias can be adjusted and even reversed easily by adjusting the phase angle between the driving frequencies and, thus, allows separate control of ion energy and flux. Furthermore, it has been found that the normalized dc self-

bias generated via the EAE is very insensitive to small changes in the amplitudes of the applied voltage waveform around the optimum voltage ratio. Thus, if a discharge is operated at the optimum voltage ratio for controlling the ion energy separately from the ion flux, a high degree of process stability with respect to small changes in the applied voltages is expected; i.e., the ion energy will remain fairly constant.

VII. ACKNOWLEDGMENTS

This work has been funded by the DFG through Grant No. GRK 1051, by the Ruhr University Research School, and by the Hungarian Fund for Scientific Research Grant Nos. OTKA-T048389 and OTKA-K77653.

[1]M. A. Lieberman and A. J. Lichtenberg, *Principles of Plasma Discharges and Materials Processing*, 2nd ed. (Wiley Interscience, NJ, 2005).
[2]P. C. Boyle, A. R. Ellingboe, and M. M. Turner, Plasma Sources Sci. Technol. **13**, 493 (2004).
[3]P. C. Boyle, A. R. Ellingboe, and M. M. Turner, J. Phys. D **37**, 697 (2004).
[4]T. Kitajima, Y. Takeo, Z. L. Petrović, and T. Makabe, Appl. Phys. Lett. **77**, 489 (2000).
[5]T. Denda, Y. Miyoshi, Y. Komukai, T. Goto, Z. L. Petrović, and T. Makabe, J. Appl. Phys. **95**, 870 (2004).
[6]J. K. Lee, O. V. Manuilenko, N. Yu. Babaeva, H. C. Kim, and J. W. Shon, Plasma Sources Sci. Technol. **14**, 89 (2005).
[7]T. Gans, J. Schulze, D. O'Connell, U. Czarnetzki, R. Faulkner, A. R. Ellingboe, and M. M. Turner, Appl. Phys. Lett. **89**, 261502 (2006).
[8]J. Schulze, T. Gans, D. O'Connell, U. Czarnetzki, A. R. Ellingboe, and M. M. Turner, J. Phys. D **40**, 7008 (2007).
[9]J. Schulze, Z. Donkó, D. Luggenhölscher, and U. Czarnetzki, Plasma Sources Sci. Technol. **18**, 034011 (2009).
[10]E. Kawamura, M. A. Lieberman, and A. J. Lichtenberg, Phys. Plasmas **13**, 053506 (2006).
[11]M. M. Turner and P. Chabert, Phys. Rev. Lett. **96**, 205001 (2006).
[12]D. O'Connell, T. Gans, E. Semmler, and P. Awakowicz, Appl. Phys. Lett. **93**, 081502 (2008).
[13]Z. Donkó and Z. Lj. Petrović, Jpn. J. Appl. Phys., Part 1 **45**, 8151 (2006).
[14]J. W. Coburn and E. Kay, J. Appl. Phys. **43**, 4965 (1972).
[15]K. Kohler, J. W. Coburn, D. E. Horne, E. Kay, and H. Keller, J. Appl. Phys. **57**, 59 (1985).
[16]Y. P. Song, D. Field, and D. F. Klemperer, J. Phys. D **23**, 673 (1990).
[17]M. A. Lieberman and S. E. Savas, J. Vac. Sci. Technol. A **8**, 1632 (1990).
[18]J. Schulze, B. G. Heil, D. Luggenhölscher, U. Czarnetzki, and R. P. Brinkmann J. Phys. D **41**, 042003 (2008).
[19]J. Schulze, B. G. Heil, D. Luggenhölscher, and U. Czarnetzki, IEEE Trans. Plasma Sci. **36**, 1400 (2008).
[20]J. Schulze, B. G. Heil, D. Luggenhölscher, R. P. Brinkmann, and U. Czarnetzki, J. Phys. D **41**, 195212 (2008).
[21]B. G. Heil, J. Schulze, T. Mussenbrock, R. P. Brinkmann, and U. Czarnetzki, IEEE Trans. Plasma Sci. **36**, 1404 (2008).
[22]B. G. Heil, U. Czarnetzki, R. P. Brinkmann, and T. Mussenbrock, J. Phys. D **41**, 165202 (2008).
[23]U. Czarnetzki, B. G. Heil, J. Schulze, Z. Donkó, T. Mussenbrock, and R. P. Brinkmann, J. Phys.: Conf. Ser. **162**, 012010 (2009).
[24]Z. Donkó, J. Schulze, B. G. Heil, and U. Czarnetzki, J. Phys. D **42**, 025205 (2009).
[25]J. Schulze, E. Schüngel, Z. Donkó, and U. Czarnetzki J. Phys. D **42**, 092005 (2009).
[26]Z. Donkó, J. Schulze, U. Czarnetzki, and D. Luggenhölscher, Appl. Phys. Lett. **94**, 131501 (2009).
[27]S. Longo and P. Diomede, Plasma Processes Polym. **6**, 370 (2009).
[28]A. V. Phelps and Z. Lj. Petrović, Plasma Sources Sci. Technol. **8**, R21 (1999).
[29]A. V. Phelps, J. Appl. Phys. **76**, 747 (1994).
[30]A. V. Phelps, http://jilawww.colorado.edu/~avp/collision_data/
[31]J. Schulze, Z. Donkó, B. G. Heil, D. Luggenhölscher, T. Mussenbrock, R. P. Brinkmann, and U. Czarnetzki, J. Phys. D **41**, 105214 (2008).
[32]Z. Donkó and Z. Lj. Petrović, J. Phys.: Conf. Ser. **86**, 012011 (2007).